PAPER • OPEN ACCESS

Multidimensional measures of electromagnetic chirality and their conformal invariance

To cite this article: Maxim Vavilin and Ivan Fernandez-Corbaton 2022 *New J. Phys.* **24** 033022

View the article online for updates and enhancements.

CrossMark

PAPER

Multidimensional measures of electromagnetic chirality and their conformal invariance

Maxim Vavilin[1],[*] 🄳 and Ivan Fernandez-Corbaton[2] 🄳

1   Institute of Theoretical Solid State Physics, Karlsruhe Institute of Technology, Karlsruhe, Germany
2   Institute of Nanotechnology, Karlsruhe Institute of Technology, Karlsruhe, Germany
*   Author to whom any correspondence should be addressed.

E-mail: maxim.vavilin@kit.edu

Abstract

Proper assignment of left- and right-handed labels to general chiral objects is known to be a theoretically unfeasible problem. Attempts to utilize a pseudoscalar function to distinguish enantiomers face two unavoidable difficulties: false chiral zeros and unhanded chiral states. In here, we demonstrate how both of these problems can be solved in the context of light–matter interactions. First, we introduce a two-dimensional quantity called complex electromagnetic chirality that solves the problem of false chiral zeros. Next, we define an infinite-dimensional pseudovector called chirality signature that completely quantifies the multidimensional nature of electromagnetic chirality, does not have false global chiral zeros, and allows to continuously distinguish any pair of enantiomers because it does not produce unhanded chiral states. We prove that the introduced measures are invariant under the largest group of symmetries of Maxwell's equations—the conformal group. The complete, continuous, and conformally invariant quantification of electromagnetic chirality provided by the chirality signature distinguishes it as a particularly suitable tool for the study of chirality and its applications.

1. Introduction

There are two types of objects: those that can be superimposed onto their own mirror image and those that cannot. The latter are called chiral objects and they exist in pairs (called enantiomers): an object and its mirror antipode. One often distinguishes between both versions by assigning a discrete label 'left' or 'right' using a reference or a conventional rule. There are hence two different albeit related concepts: chirality, which is a property of an object to differ from its mirror image, and handedness, which is a label that tells two enantiomers apart.

The concept of chirality underlies a wide spectrum of physical phenomena, ranging from the left-right asymmetry of the weak interaction in particle physics, through the differential response of chiral molecules to different polarization handedness of light, to chiral magnetic fields of galactic scale. Practical aspects of selecting a particular molecular enantiomer are crucial in pharmacy, for example when both left and right-handed versions of the same chiral molecule are produced in a chemical reaction, but only one has the required medical effect.

It is remarkable that, despite their broad use, the left and right-handed labels cannot be appropriately assigned to all chiral objects [1, 2]. A chiral object that is complex enough can be transformed into its mirror image by a continuous transformation such that it stays chiral at all times [3, 4]. This is known as the chiral connectedness property, and is the source of two main difficulties in the quantitative studies of chirality: false chiral zeros, and unhanded states.

Attempts to quantify chirality with a continuous real pseudoscalar function face the unsolvable difficulty of false chiral zeros. Under the requirement that such function obtains the value of zero for achiral states and takes values of opposite signs for enantiomeric configurations, the chiral connectedness implies that the function would also have to acquire a value of zero for some chiral configuration [5]. In this case one speaks

of a false chiral zero—the zero value of the pseudoscalar function cannot definitively indicate an achiral state. Moreover, there are strong indications that the use of two (or several) pseudoscalar functions does not resolve the problem of false chiral zeros either. Since even objects as simple as tetrahedra are chiraly connected [4], assuming that a pair or pseudoscalar functions exists which never have chiral zeros simultaneously for arbitrarily complex physical objects is equivalent to assuming that the subset of objects that have zero value of the first pseudoscalar function is *not* chiraly connected, i.e. that such subset is more primitive than the set of tetrahedrons. This is unsound, since only one degree of freedom was removed. The argument can be repeated after including more pseudoscalars. Notably, a precise recipe specifying and demonstrating a fixed finite set of pseudoscalars that are defined on a general set of physical objects and never share false chiral zeros has never been put forward.

The second, more general problem that follows from chiral connectedness is the problem of unhanded states: a pseudoscalar function cannot be used to assign handedness labels 'left' or 'right' to all objects [1]. There are chiral configurations at which the function vanishes (due to chiral connectedness), which are called unhanded configurations, unhanded states, or states of latent handedness. In other words, there is a deficiency in enantiomeric differentiation: there are pairs of chiral objects, one mirror image of the other and physically different, that cannot be distinguished using one (or several) fixed pseudoscalar functions.

The problem of unhanded states attracted interest in chemistry, for example Pinto *et al* in [2] proposed an abstract strategy of assigning a handedness label 'left' or 'right' that does not give rise to unhanded states for chiral objects. Their idea consists in constructing a hierarchy of rules, each assigning a left, right, or unhanded label. Then, applying the rules consecutively until some rule determines the given object as left or right (i.e. not unhanded), one identifies the handedness of the object with this result. The emergence of such hierarchical constructions indicates the multi-dimensional nature of chirality. A precise definition of quantitative chirality measures reflecting such multi-dimensionality was so far lacking.

The purpose of this paper is to solve both the false chiral zeros problem, and the unhanded states problem in the context of light–matter interactions, by providing continuous quantitative descriptions of chirality. For this we study the chirality of objects by reference to their interaction with the electromagnetic field. We do not focus on individual chiral properties such as optical rotation or circular dichroism, but instead we use the T-matrix method [6, 7]. The T-matrix (or transition matrix) contains the complete information about the linear interaction of an object with dynamic electromagnetic fields, allowing to formalize chirality measures as functions on the spaces of T-matrices. Additionally, there is an abundance of resources that numerically compute T-matrices of various systems [8], including the calculation of T-matrices for molecules from quantum-mechanical simulation data [9].

Previously [10], the use of the T-matrix method allowed to reinterpret chirality in the context of light–matter interactions by measuring how differently the object interacts with fields of opposite polarization handedness. The new property was called electromagnetic chirality (em-chirality), and its scalar measure was introduced as well. This measure has an upper bound with the remarkable characteristic that maximally em-chiral reciprocal objects are invisible to all light of a particular polarization handedness. Efforts to design and fabricate materials with such properties are ongoing [11–13]. The notion of em-chirality is also being considered in applied mathematics [14, 15].

To solve the problem of quantification of handedness without false chiral zeros we consider one particular pseudoscalar property of a scatterer and combine it with the scalar measure of em-chirality. We render the result as a complex-valued function called complex em-chirality. It features the scalar em-chirality as its absolute value and the pseudoscalar function as its real part. Zero values of the pseudoscalar property will only contribute to the zero value of the real part of the complex number—the question whether an object is chiral or achiral is then addressed by the absolute value, which allows to separate achiral states from unhanded states.

Next, we solve the problem of unhanded states by providing the complete description of em-chirality that allows to continuously distinguish any two enantiomers. We introduce an infinite-dimensional pseudovector called chirality signature, whose pseudoscalar components vanish simultaneously if and only if the configuration is em-achiral. This provides, for the first time, the complete quantification of the multidimensional nature of chirality in light–matter interactions. Despite its infinite-dimensionality it can be practically calculated and represented, because it admits an appropriate truncation. The complete and continuous quantification of chirality is suitable for the study of chirality evolution. For example, it opens up the possibility of quantitatively studying chirality evolution in chemical reactions [2] where one molecular enantiomer converts into the other [16], or where a chiral intermediate state mediates between achiral reactants and achiral products [17].

Furthermore, we show that the chirality signature, the scalar and complex measures of em-chirality are invariant under the group of conformal transformations, which is the largest group of symmetries of Maxwell's equations. This means, in particular, that each chirality signature is uniquely associated with a corresponding set of objects, where all objects in the set are related to each other by conformal transformations.

The article is organized as follows. Sections 2 and 3 provide the context for the core sections 4–7. Section 2 contains an overview of the helicity operator and the T-matrix method, which are two central concepts for the study of electromagnetic chirality. Section 3 contains a brief exposition of the em-chirality and its scalar measure that were previously introduced in [10], including a new equivalent alternative definition of em-chirality as the solution of a Procrustes-like minimization problem. In section 4 we define the complex em-chirality and then use it in section 5 to illustrate a solution to the false chiral zeros problem. Section 6 is devoted to the chirality signature. Both sections 5 and 6 contain numerical examples that illustrate the discussions using chiral configurations of dielectric spheres in the monochromatic regime. In section 7 we prove the conformal invariance of the introduced measures. In section 8 we briefly discuss the applicability of the measures outside of electromagnetism, and section 9 contains the final remarks.

2. Helicity and the T-matrix

2.1. Electromagnetic helicity as chirality reference

When studying chirality of any object one is often interested in a reference that changes its property under mirror transformations. In the context of light–matter interactions the role of such reference is played by the polarization handedness of light, or, more fundamentally, the electromagnetic helicity. The role of helicity in chiral light–matter interactions is under intense scrutiny [18–31]. We can split any electromagnetic field into two components of opposite helicity, left-handed and right-handed, corresponding to eigenstates of the helicity operator Λ with eigenvalues $\lambda = 1$ and $\lambda = -1$, respectively. The helicity operator Λ is defined as the projection of the angular momentum operator onto the direction of the linear momentum operator

$$\Lambda = \frac{\boldsymbol{J} \cdot \boldsymbol{P}}{|\boldsymbol{P}|}. \tag{1}$$

The fundamental importance of helicity arises from the invariance of the helicity operator Λ under translations, rotations and Lorentz boosts [32, section 10.4]. This fact is embedded in the theory of special relativity: since the speed of light is maximal, it is impossible to boost a reference frame such that the photon would reverse its direction, which means that the projection of its angular momentum onto its direction cannot switch under changes of reference frames. The parity transformation, however, anticommutes with the helicity operator Λ and hence changes the sign of λ, which makes helicity a natural chirality reference in light–matter interactions. In this article we will be using the helicity basis for representing states of the electromagnetic field, and the operators describing the light–matter interactions.

In the space of solutions of Fourier-transformed Maxwell's equations in an empty source-free region the helicity operator in equation (1) is represented by the curl operator divided by the wavenumber

$$\Lambda \to \frac{1}{k} \nabla \times . \tag{2}$$

2.2. The T-matrix method

One of the most powerful and efficient methods of theoretical study of various light–matter interaction problems is the T-matrix method. Usually one considers a monochromatic electromagnetic field in the presence of a scatterer that is enclosed in a sphere of radius R around the origin. The Fourier-transformed Maxwell's equations for the empty source-free region outside of this sphere read

$$\nabla \times \boldsymbol{E} = ikZ_0\boldsymbol{H}, \qquad \nabla \times \boldsymbol{H} = -ik\boldsymbol{E}/Z_0 \tag{3}$$

$$\nabla \cdot \boldsymbol{E} = 0, \qquad \nabla \cdot \boldsymbol{H} = 0, \tag{4}$$

where $Z_0 = \mu_0 c$ is the impedance of the free space, $k = |\boldsymbol{k}| = \omega/c > 0$ is the length of the wave vector, and the harmonic time-dependence $e^{-i\omega t}$ is omitted. The general solution can be decomposed in electric $(\text{Rg}\,\boldsymbol{N}_{jm}(\boldsymbol{r}), \boldsymbol{N}_{jm}(\boldsymbol{r}))$ and magnetic $(\text{Rg}\,\boldsymbol{M}_{jm}(\boldsymbol{r}), \boldsymbol{M}_{jm}(\boldsymbol{r}))$ multipoles [7]:

$$E_{\text{tot}}(\boldsymbol{r}) = \sum_{j=1}^{\infty} \sum_{m=-j}^{j} a_{jm} \text{Rg}\,\boldsymbol{M}_{jm}(\boldsymbol{r}) + b_{jm} \text{Rg}\,\boldsymbol{N}_{jm}(\boldsymbol{r}) \tag{5}$$

$$+ \sum_{j=1}^{\infty} \sum_{m=-j}^{j} c_{jm}\,\boldsymbol{M}_{jm}(\boldsymbol{r}) + d_{jm}\,\boldsymbol{N}_{jm}(\boldsymbol{r}), \quad |\boldsymbol{r}| > R, \tag{6}$$

with

$$\text{Rg}\,\boldsymbol{M}_{jm}(\boldsymbol{r}) = j_j(kr)(-i)\boldsymbol{r} \times \nabla \frac{Y_{jm}(\theta,\phi)}{\sqrt{j(j+1)}} \tag{7}$$

$$\text{Rg}\,\boldsymbol{N}_{jm}(\boldsymbol{r}) = \frac{1}{k}\nabla \times \text{Rg}\,\boldsymbol{M}_{jm}(\boldsymbol{r}) \tag{8}$$

and

$$\text{Rg}\,\boldsymbol{M}_{jm}(\boldsymbol{r}) = \frac{1}{k}\nabla \times \text{Rg}\,\boldsymbol{N}_{jm}(\boldsymbol{r}), \tag{9}$$

where a_{jm} and b_{jm} are expansion coefficients, $j_j(\cdot)$ are spherical Bessel functions and $Y_{jm}(\theta,\phi)$ are the spherical functions as defined in [33, section 3.5].

The magnetic field is simply given by

$$\boldsymbol{H}_{\text{tot}}(\boldsymbol{r}) = \frac{i}{k}\nabla \times \boldsymbol{E}_{\text{tot}}(\boldsymbol{r}). \tag{10}$$

The irregular terms in (6), i.e. $\boldsymbol{M}_{jm}(\boldsymbol{r})$ and $\boldsymbol{N}_{jm}(\boldsymbol{r})$, are acquired by interchanging spherical Bessel functions $j_j(\cdot)$ for spherical Hankel functions of the first kind $h_j^{(1)}(\cdot)$. The regular term in (5) is called the incident field $\boldsymbol{E}_i$ and the irregular term in (6) is called the scattered field $\boldsymbol{E}_s$.

The complete information about linear interaction of an object with dynamic electromagnetic fields is contained in its T-matrix [7]. It connects the coefficients of the incident and the scattered fields:

$$T\begin{pmatrix}\vec{a} \\ \vec{b}\end{pmatrix} = \begin{pmatrix}\vec{c} \\ \vec{d}\end{pmatrix}, \tag{11}$$

where $\vec{a}$, $\vec{b}$, $\vec{c}$, and $\vec{d}$ are composed of the coefficients a_{jm}, b_{jm}, c_{jm}, and d_{jm}, respectively. The T-matrix is connected to the scattering (S) matrix by the relation $S = 1 + 2T$ and provides an equivalent description.

While the T-matrix is most often considered for monochromatic fields, group-theoretical arguments allow the generalization to polychromatic fields. Such generalization will be the subject of a dedicated article. Here we describe a few aspects that are necessary for the present article.

First, we change the multipole basis to a multipole basis of eigenstates of the helicity operator:

$$\text{Rg}\,\boldsymbol{A}_{\lambda jm}(\boldsymbol{r},\omega) := \frac{1}{\sqrt{2}}\left(\text{Rg}\,\boldsymbol{M}_{jm}(\boldsymbol{r},\omega) + \lambda \text{Rg}\,\boldsymbol{N}_{jm}(\boldsymbol{r},\omega)\right) \tag{12}$$

for helicity $\lambda = \pm 1$. The property

$$\frac{\nabla}{k} \times \text{Rg}\,\boldsymbol{A}_{\lambda jm}(\boldsymbol{r},\omega) = \lambda \text{Rg}\,\boldsymbol{A}_{\lambda jm}(\boldsymbol{r},\omega) \tag{13}$$

follows from (8) and (9).

Next, we use the results of [34, equations (33b) and (33c)] to write the incident polychromatic field as

$$\boldsymbol{E}_i(\boldsymbol{r},t) = \sum_{\lambda=\pm 1} \sum_{j=1}^{\infty} \sum_{m=-j}^{j} \int_{>0}^{\infty} \mathrm{d}\omega\,\omega(i)^{j-1} f_{jm\lambda}(\omega)\text{Rg}\,\boldsymbol{A}_{\lambda jm}(\boldsymbol{r},\omega)\mathrm{e}^{-i\omega t}. \tag{14}$$

The main advantage of this representation lies in the transformation properties of the coefficients $f_{jm\lambda}(\omega) \propto a_{jm} + \lambda b_{jm}$. As discussed in [34], they transform under unitary irreducible representations of the Poincaré group for zero mass and helicity $\lambda = \pm 1$ in the multipolar basis. In particular, each helicity eigenstate transforms independently. That is, the two helicities do not mix upon transformations of the Poincaré group. We will use these transformations properties for proving invariance properties of em-chirality in section 7. We also note that the scattered field (6) can be written in the same form as equation (14) by exchanging $j_j(\cdot)$ for $h_j^{(1)}(\cdot)$. Transformation properties of the scattered field coefficients are the same as of the incident field, since spherical Hankel functions are defined by the same differential equations as the spherical Bessel functions [35]. The T-matrix can now be re-interpreted as an operator that acts in the Hilbert space of irreducible representations of the Poincaré group labeled by zero mass and helicity $\lambda = \pm 1$. A state in this space can be written as [34]:

$$|f\rangle = \sum_{\lambda=\pm1} \sum_{j=1}^{\infty} \sum_{m=-j}^{j} \int_{>0}^{\infty} \frac{\mathrm{d}\omega}{\omega} f_{jm\lambda}(\omega)|\omega jm\lambda\rangle \tag{15}$$

$$= \sum_{\lambda=\pm1} \int \frac{\mathrm{d}^3\boldsymbol{p}}{|\boldsymbol{p}|} f_\lambda(\boldsymbol{p})|\boldsymbol{p}\lambda\rangle. \tag{16}$$

Equation (15) is the decomposition in the multipolar basis states, also known as angular momentum basis states $|\omega jm\lambda\rangle$, which are eigenvectors of four operators $\boldsymbol{P}^2$, J^2, J_3 and Λ, while equation (16) is the decomposition in the plane wave basis where $|\boldsymbol{p}\lambda\rangle$ are eigenvectors of P_1, P_2, P_3, and Λ. The state functions are square-integrable with respect to the scalar product

$$\langle f|h\rangle = \sum_{\lambda=\pm1} \sum_{j=1}^{\infty} \sum_{m=-j}^{j} \int_{>0}^{\infty} \frac{\mathrm{d}\omega}{\omega} f_{jm\lambda}^*(\omega) h_{jm\lambda}(\omega), \tag{17}$$

whose equivalent expression in the plane-wave basis is

$$\langle f|h\rangle = \sum_{\lambda=\pm1} \int \frac{\mathrm{d}^3\boldsymbol{p}}{|\boldsymbol{p}|} f_\lambda^*(\boldsymbol{p}) h_\lambda(\boldsymbol{p}). \tag{18}$$

The value of $\langle f|h\rangle$ is invariant under the action of the Poincaré group. In fact, Gross [36] showed that this scalar product is also invariant under the conformal group—the largest group of symmetries of Maxwell's equations. The conformal group extends the Poincaré group with dilations and special conformal transformations. This means that, for any operator X representing a transformation of the conformal group, such as e.g. a Lorentz boost, and for any pair of states $|f\rangle$ and $|h\rangle$, we have that the inner-product of the transformed states $X|f\rangle$, and $X|h\rangle$ is equal to the inner-product of the original states: $\langle f|h\rangle = \langle f|X^\dagger X|h\rangle$, implying the unitarity of X.

It is straightforward to restrict the generalized polychromatic T-operator to a single-frequency description, recovering the common monochromatic T-matrix. One benefit of the polychromatic description consists in the ability to describe objects that change the frequencies in the scattering process, such as in Raman scattering. Moreover, the general T-operator is necessary for considering Lorentz transformations, dilations, and special conformal transformations, since all these transformations change the frequency content of the electromagnetic field.

3. Electromagnetic chirality

Since the linear interaction of a scatterer with dynamic electromagnetic fields is completely described by its T-operator, it is essential to define chirality as a function on the space of T-operators. In [10], the T-operator approach allowed to introduce the notion of *electromagnetic chirality* (em-chirality) and its scalar measure, which reflects how differently the object interacts with fields of opposite helicity. In this interpretation chirality becomes a Lorentz-invariant property that includes the usual geometric chirality as a special case. The scalar measure of em-chirality admits a maximal value that depends on the total interaction of the object with the electromagnetic field. Objects that achieve the maximal value are invisible to all fields of a particular polarization handedness. In this section we provide a short exposition of the corresponding results.

A T-operator in the helicity basis

$$T = \begin{pmatrix} T^{++} & T^{+-} \\ T^{-+} & T^{--} \end{pmatrix} \tag{19}$$

consists of four suboperators $T^{\lambda\lambda'}$ that act on states with helicity $\lambda' = \pm1$ and map them to states with helicity $\lambda = \pm1$. Electromagnetically achiral objects are defined as those that satisfy

$$T^{++} = U_1 T^{--} V_1^\dagger \tag{20}$$

$$T^{-+} = U_2 T^{+-} V_2^\dagger \tag{21}$$

for some unitary $U_{1,2}$ and $V_{1,2}$. When conditions (20) and (21) are met, the measurements done with incident fields of a particular polarization handedness are unitarily similar to the measurements done with incident fields of the opposite polarization handedness [10], and hence do not provide new information.

The definition of em-chirality contains the common geometric definition of chirality, because translations and rotations act unitarily on the T-suboperators and do not change the polarization handedness of the EM-field.

But since the set of unitary transformations is larger than the set of rotations and translations, there exist geometrically chiral objects that are not electromagnetically chiral, for example those that fulfill equations (20) and (21) with Lorentz transformations and not with rotations or translations.

To answer the question, to which degree a given scatterer is electromagnetically chiral, the scalar measure of em-chirality χ was introduced in [10] using the sequences of singular values of the suboperators[3]:

$$\chi(T) = \sqrt{\sum_k (\sigma_k(T^{++}) - \sigma_k(T^{--}))^2 + \sum_k (\sigma_k(T^{+-}) - \sigma_k(T^{-+}))^2} \qquad (22)$$

$$=: \sqrt{|\vec{\sigma}(T^{++}) - \vec{\sigma}(T^{--})|^2 + |\vec{\sigma}(T^{+-}) - \vec{\sigma}(T^{-+})|^2}, \qquad (23)$$

where $\vec{\sigma}(A)$ denotes the non-increasing sequence of singular values of A. For future reference we also define the following dot product operator:

$$\vec{\sigma}(A) \cdot \vec{\sigma}(B) = \sum_{k=0}^{\infty} \sigma_k(A)\sigma_k(B). \qquad (24)$$

The T-suboperators in equation (23) are assumed to have finite Hilbert–Schmidt norm

$$\left\| T^{\lambda\lambda'} \right\|_{\mathrm{HS}}^2 := \int \frac{\mathrm{d}^3 \boldsymbol{p}}{|\boldsymbol{p}|} \frac{\mathrm{d}^3 \boldsymbol{p}'}{|\boldsymbol{p}'|} \left| T^{\lambda\lambda'}(\boldsymbol{p}, \boldsymbol{p}') \right|^2 < \infty, \qquad (25)$$

which ensures the existence of their singular value decomposition (SVD). Then, we have that

$$\left\| T^{\lambda\lambda'} \right\|_{\mathrm{HS}}^2 = \vec{\sigma}(T^{\lambda\lambda'}) \cdot \vec{\sigma}(T^{\lambda\lambda'}). \qquad (26)$$

Using the von Neumann trace inequality for Hilbert–Schmidt operators [37] we re-write the definition of em-chirality in equation (23) (see appendix A) as

$$\chi(T) = \sqrt{\min_{U_1 V_1} \| T^{++} - U_1 T^{--} V_1^\dagger \|_{\mathrm{HS}}^2 + \min_{U_2 V_2} \| T^{-+} - U_2 T^{+-} V_2^\dagger \|_{\mathrm{HS}}^2}, \qquad (27)$$

where the minimization is performed with respect to all unitary $U_{1,2}$ and $V_{1,2}$. Taking into account section 2, we note that this definition can be applied to both single-frequency scattering and to scattering taking place in the whole frequency domain, in case the Hilbert–Schmidt norm of the T-operator is finite.

This measure of em-chirality is bounded by the square root of the total interaction $C_{\mathrm{int}} = \sum_{\lambda,\lambda'} \left\| T^{\lambda\lambda'} \right\|_{\mathrm{HS}}^2$, which means that χ can be normalized to take values on the unit interval $\hat{\chi} = \frac{\chi}{\sqrt{C_{\mathrm{int}}}} \in [0, 1]$. Objects that are transparent to all fields of a particular helicity necessarily exhibit maximal em-chirality $\hat{\chi} = 1$ [10], where the hat denotes the normalized version of the definition. Further properties hold for reciprocal scatterers.

3.1. Reciprocal case
Reciprocity of a scatterer reflects the symmetry of measurement results under the exchange of the source and the detector. The reciprocity condition is defined in the plane wave basis as [38, equation (2.22)]

$$\langle \boldsymbol{p}\lambda | T | \boldsymbol{p}'\lambda' \rangle = \langle -\boldsymbol{p}'\lambda' | T | -\boldsymbol{p}\lambda \rangle. \qquad (28)$$

Most usual scatterers fulfill the reciprocity condition (there are exceptions, however, such as magneto-optical materials), which makes the following properties useful in numerous applications.

Consider a SVD of T^{+-} in the plane wave basis

$$T^{+-}(\boldsymbol{p}, \boldsymbol{q}) = \sum_{k=1}^{\infty} \sigma_k \psi_k^*(\boldsymbol{p}) \phi_k(\boldsymbol{q}) \qquad (29)$$

---

[3] The singular value decomposition (SVD) of a compact operator is defined as

$$T^{\lambda\lambda'} = \sum_{k=1}^{\infty} \sigma_k(T^{\lambda\lambda'}) |\psi_k\rangle\langle\phi_k|$$

with a unique sequence of non-increasing singular values $\sigma_k(T^{\lambda\lambda'})$ and some families of orthonormal vectors $|\psi_k\rangle$ and $|\phi_k\rangle$.

for some orthonormal families of states $|\psi_k\rangle$ and $|\phi_k\rangle$. Then it follows from equation (28) that

$$T^{-+}(\boldsymbol{p},\boldsymbol{q}) = T^{+-}(-\boldsymbol{q},-\boldsymbol{p}) = \sum_{k=1}^{\infty} \sigma_k\,\psi_k^*(-\boldsymbol{q})\,\phi_k(-\boldsymbol{p}) = \sum_{k=1}^{\infty} \sigma_k\,\xi_k^*(\boldsymbol{p})\,\mu_k(\boldsymbol{q}) \tag{30}$$

for orthonormal families $\xi_k(\boldsymbol{p}) := \phi_k^*(-\boldsymbol{p})$ and $\mu_k(\boldsymbol{q}) := \psi_k^*(-\boldsymbol{q})$. It implies that the sequences of singular values of T^{+-} and T^{-+} are equal

$$\vec{\sigma}(T^{+-}) - \vec{\sigma}(T^{-+}) = \vec{0} \tag{31}$$

and the second term of equation (23) vanishes, which can be used to simplify computations.

Another property is reflected in the fact that a reciprocal object that exhibits the maximum value of normalized scalar em-chirality $\hat{\chi} = 1$ is transparent to fields of either positive or negative polarization handedness. The proof of this fact can be found in [10].

4. Complex em-chirality

Now we attempt to assign left- or right handedness to an em-chiral object. As argued in [1], no pseudoscalar property can be used for defining a proper left–right classification of general chiral objects in terms of a real number that acquires opposite signs for enantiomers and that is zero only for an *achiral* object. Most classes of objects possess the so-called chiral connectedness property, which means that chiral objects can be continuously transformed into their mirror enantiomers while staying chiral during the transformation. Then, in accordance with the intermediate value theorem, the pseudoscalar function must take a zero value at some point, which would nevertheless correspond to a *chiral* configuration. In such case one speaks of a false chiral zero.

In this subsection we show how a combination of a pseudoscalar property with a scalar chirality measure can solve the problem of false chiral zeros. We extend the normalized scalar measure of em-chirality by multiplying it with a complex exponential phase factor. The latter depends on the difference in interaction cross-sections of fields of opposite polarization handedness, which is a pseudoscalar property. The complex em-chirality is defined as

$$\chi_c(T) = \hat{\chi}(T)\exp(i\phi(T)), \tag{32}$$

where

$$\phi(T) := -\frac{\pi}{2}\left(\frac{\|T^{++}\|^2 + \|T^{-+}\|^2 - \|T^{+-}\|^2 - \|T^{--}\|^2}{\|T\|^2} - 1\right) \tag{33}$$

$$= \pi\frac{\|T^{+-}\|^2 + \|T^{--}\|^2}{\|T\|^2} \in [0,\pi] \tag{34}$$

and the Hilbert–Schmidt norm is implied. The absolute value of the complex em-chirality is the normalized scalar em-chirality $|\chi_c(T)| = \hat{\chi}(T)$ and the real part $\mathfrak{R}(\chi_c)$ will be referred to as the handedness measure of the scatterer.

The defining property of the phase factor consists in its behavior under arbitrary mirror transformations. The T-matrix is transformed as

$$\begin{pmatrix} T^{++} & T^{+-} \\ T^{-+} & T^{--} \end{pmatrix} \to \begin{pmatrix} \widetilde{T}^{--} & \widetilde{T}^{-+} \\ \widetilde{T}^{+-} & \widetilde{T}^{++} \end{pmatrix}, \tag{35}$$

where tilde indicates a reflection of a T-suboperator, which is a unitary transformation. The permutation of suboperators is due to the change of the helicity under mirror transformations.

The phase of the complex em-chirality ϕ changes under mirror transformations according to

$$\phi(T) = \pi\frac{\|T^{+-}\|^2 + \|T^{--}\|^2}{\|T\|^2} \to \pi\frac{\|T^{-+}\|^2 + \|T^{++}\|^2}{\|T\|^2} \tag{36}$$

$$= \pi\frac{\|T\|^2 - \|T^{+-}\|^2 - \|T^{--}\|^2}{\|T\|^2} \tag{37}$$

$$= \pi - \phi(T), \tag{38}$$
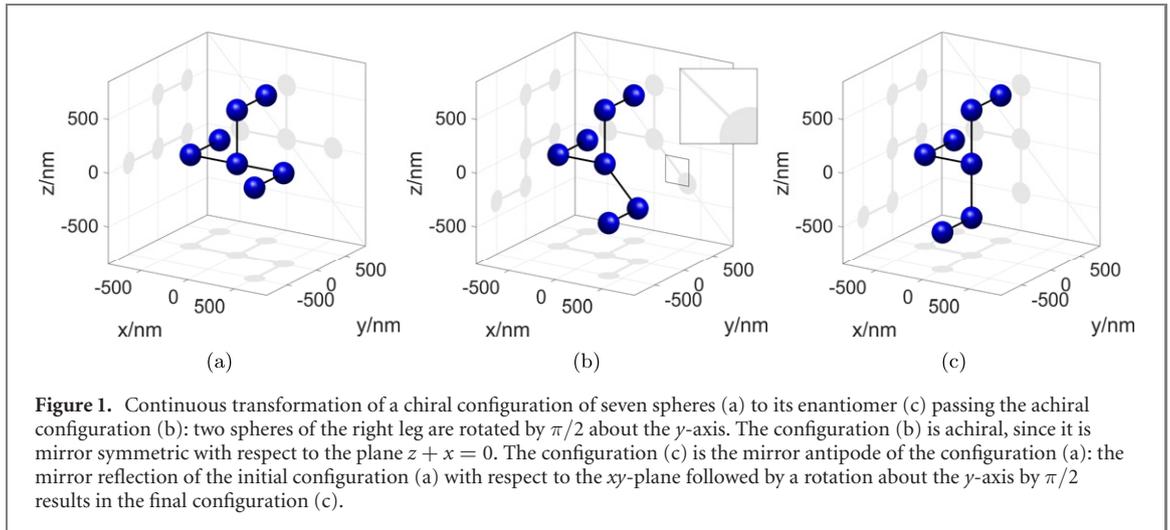
Figure 1. Continuous transformation of a chiral configuration of seven spheres (a) to its enantiomer (c) passing the achiral configuration (b): two spheres of the right leg are rotated by $\pi/2$ about the y-axis. The configuration (b) is achiral, since it is mirror symmetric with respect to the plane $z + x = 0$. The configuration (c) is the mirror antipode of the configuration (a): the mirror reflection of the initial configuration (a) with respect to the xy-plane followed by a rotation about the y-axis by $\pi/2$ results in the final configuration (c).

so the mirror transformation reflects the complex em-chirality with respect to the imaginary axis

$$\hat{\chi}(T) \exp(\mathrm{i}\phi(T)) \rightarrow \hat{\chi}(T) \exp(\mathrm{i}(\pi - \phi(T))), \tag{39}$$

which changes the sign of the handedness.

The complex em-chirality maps a scatterer to a semicircle of unit radius, which is divided into four distinct regions: of right-handed $\mathfrak{R}(\chi_c) < 0$, left-handed $\mathfrak{R}(\chi_c) > 0$, achiral $\chi_c = 0$, and unhanded $\mathfrak{R}(\chi_c) = 0$, $\chi_c \neq 0$ scatterers. This allows to distinguish between unhanded and achiral states, which constitutes the solution to the false chiral zeros problem.

Just as with the scalar em-chirality, the complex em-chirality can be defined for T-operators acting on the whole frequency domain as well as T-matrices describing monochromatic scattering. In the former case it becomes possible to define handedness for frequency-mixing scatterers. In section 5 we apply complex em-chirality in the monochromatic regime for a numerical illustration of chiral connectedness and the false chiral zeros problem. Appendix B contains further properties of complex em-chirality. In particular, that $\chi_c(T) = 1(-1)$ for objects that are invisible to light of negative(positive) helicity.

One limitation of the complex em-chirality consists in the existence of unhanded states. This implies that there are pairs of enantiomers that have the same value of complex em-chirality, and therefore cannot be distinguished by χ_c. This problem is integral to all approaches that try to distinguish enantiomers by assigning left- and right-handed labels, which is in general not sufficient to describe the complete multidimensional nature of chirality [1, 2]. Besides, the choice of the pseudoscalar property is rather arbitrary, so alternative pseudoscalar properties would lead to a different assignment of handedness labels. The alternative approach to analyzing chirality and distinguishing enantiomers that is free of such drawbacks will be discussed in section 6.

5. Illustration of chiral connectedness with complex em-chirality and solution to the false chiral zero problem

We apply the notion of complex em-chirality to study a reciprocal system of seven dielectric spheres and its continuous transformations. We start with a geometrically chiral composition of spheres with radii $r = 100$ nm and relative permittivity $\epsilon_r^s = 4$ in air ($\epsilon_r^{air} = 1$) that are centered at points $(-a, a, 0)$, $(-a, 0, 0)$, $(0, 0, 0)$, $(0, 0, a)$, $(0, a, a)$, $(a, 0, 0)$ and $(a, -a, 0)$, with $a = 500$ nm as shown in figure 1(a). The last two spheres (the right leg of the configuration) will be continuously rotated around the y-axis until a maximal rotation angle of $\pi/2$ in the positive direction, where the configuration of figure 1(c) is reached. The final state is the enantiomer of the initial one. This can be seen by reflecting the starting configuration with respect to the xy-plane and then rotating the resulting object about the y-axis by $\pi/2$.

We consider electromagnetic scattering properties of spheres at a fixed frequency $f = 500$ THz and calculate the T-matrix of the configuration at numerous points of the continuous transformation using a typical multiscattering algorithm [39], which is implemented in the code described in [40]. This allows to numerically compute the trajectory of the complex em-chirality χ_c for this process, the result of which is presented in figure 3(a). The starting configuration is right-handed $\mathfrak{R}(\chi_c) < 0$ and the final configuration is left-handed $\mathfrak{R}(\chi_c) > 0$. The zero value of complex em-chirality corresponds to the arrangement of

Figure 2. Continuous transformation of the initial chiral configuration (a) to its enantiomer (f) avoiding any intermediate achiral configuration. The transformation is similar to the of figure 1, but the achiral state figure 1(b) is avoided as follows. First, the right leg is rotated about the *y*-axis by $9\pi/40$ (b). Then, the furthest top sphere is shifted by 50 nm along the negative direction of the *y*-axis (c)—the transparent blue sphere depicts the position of the sphere before the shift (also enlarged in the top right corner). Then the right leg is rotated by extra $2\pi/40$ (d). Afterwards the shifted top sphere is brought back to its initial position (e) and finally the right leg is rotated by the remaining $9\pi/40$ onto the final configuration. Configurations (b) and (e) are chiral, contrary to the configuration in figure 1(b). This can be clearly seen in the corresponding insets containing zoomed-in versions of the shadows of the right leg on the *y*–*z* plane. In (b) and (e) here, such shadow does not coincide with the reference diagonal, breaking the mirror symmetry that can be seen in figure 1(b).

figure 1(b), which is geometrically achiral because of its obvious mirror symmetry. As mentioned in section 3, geometrically achiral objects are electromagnetically achiral, which is the reason for vanishing χ_c.

There are, however, principally different transformations that mutate the initial state figure 1(a) into its antipode figure 1(c) without ever reaching an achiral configuration. An example of such transformation is described on figure 2. This transformation is designed to avoid achiral arrangements by breaking the mirror symmetry of figure 1(b). The corresponding trajectory of complex em-chirality on figure 3(b) shows that at no point of this transformation the configuration becomes electromagnetically achiral. The existence of such transformations is the essence of the chiral connectedness property.

If we focus solely on the handedness part, we note that it takes a zero value at the intersection of the trajectory with the imaginary line. This point is the false chiral zero of the pseudoscalar function $\mathfrak{R}(\chi_c)$. Its combination with the scalar measure of em-chirality allows to unambiguously distinguish between achiral states $|\chi_c| = 0$ and states with $\mathfrak{R}(\chi_c) = 0$, which constitutes the solution to the false chiral zero problem.

Configurations with $|\chi_c| \neq 0$ and $\mathfrak{R}(\chi_c) = 0$ can be called unhanded, because the given pseudoscalar function fails to assign a handedness to them. Such configurations are chiral, so they exist in two enantiomeric versions, but they cannot be distinguished using complex em-chirality. In the next section we provide the solution to the problem of the complete description of em-chirality, which will allow to distinguish *any* pair of enantiomers by classifying objects with respect to their chirality signature.

6. Chirality signature

The existence of chiral unhanded states $\chi_c \neq 0$, $\mathfrak{R}(\chi_c) = 0$ reveals the fact that complex em-chirality does not contain the full information about chiral properties of an object. The complete picture would be described by a mathematical object χ_s that, for an object T and its mirror antipode $\widetilde{T}$, fulfills the properties

$$\chi_s(T) = -\chi_s(\widetilde{T}) \tag{40}$$

$$T \text{ is em-achiral} \Rightarrow \chi_s(T) = 0 \tag{41}$$

$$\chi_s(T) = 0 \Rightarrow T \text{ is em-achiral} \tag{42}$$

Figure 3. Trajectories of complex em-chirality for (a) the continuous transformation that passes the achiral configuration (corresponds to figures 1) and (b) the continuous transformation that avoids the achiral configuration (corresponds to figure 2). The trajectories start in the left-handed region $\Re(\chi_c) < 0$ and end in the right-handed region $\Re(\chi_c) > 0$. The absolute value of χ_c equals the scalar em-chirality and the real part is the pseudoscalar handedness measure.

Violation of equation (42) by the handedness part of the complex em-chirality $\Re(\chi_c)$ is the cause of unhanded states.

In our framework it is possible to define a quantity that would fulfill the properties (40)–(42). Consider the difference of the sequences of singular values

$$\vec{\chi}_1(T) := \vec{\sigma}(T^{++}) - \vec{\sigma}(T^{--}) \tag{43}$$

$$\vec{\chi}_2(T) := \vec{\sigma}(T^{+-}) - \vec{\sigma}(T^{-+}). \tag{44}$$

According to equation (35) and the corresponding discussion, a mirror transformation changes the sign of each element of the sequences (43)–(44):

$$\vec{\chi}_1(\widetilde{T}) = \vec{\sigma}(T^{--}) - \vec{\sigma}(T^{++}) = -\vec{\chi}_1(T) \tag{45}$$

$$\vec{\chi}_2(\widetilde{T}) = \vec{\sigma}(T^{-+}) - \vec{\sigma}(T^{+-}) = -\vec{\chi}_2(T). \tag{46}$$

Besides, the achirality condition (20) and (21) is equivalent to $\vec{\chi}_1(T) = \vec{\chi}_2(T) = \vec{0}$. This implies that the properties (40)–(42) are fulfilled by the tuple

$$\vec{\chi}_s(T) := (\vec{\chi}_1(T), \vec{\chi}_2(T)), \tag{47}$$

which we will call the *chirality signature*.

The scalar em-chirality (equation (23)) can be written as a function of $\vec{\chi}_s(T)$ as

$$\chi = \sqrt{\vec{\chi}_1(T) \cdot \vec{\chi}_1(T) + \vec{\chi}_2(T) \cdot \vec{\chi}_2(T)}. \tag{48}$$

In the case of a reciprocal scatterer (31) the second part of the tuple vanishes

$$\vec{\chi}_2(T) = \vec{0}, \tag{49}$$

and the chirality signature may be identified just with the sequence $\vec{\chi}_1$

$$\vec{\chi}_s(T) := \vec{\chi}_1(T). \tag{50}$$

We provide an illustration for this definition using the reciprocal system from the previous section. The values of $\vec{\chi}_s(T_a)$, $\vec{\chi}_s(T_b)$ and $\vec{\chi}_s(T_c)$ are shown in figure 4, where the T-matrices correspond to the configurations described on figures 1(a)–(c).

Figure 4. First 70 components of the chirality signature for the initial T_a, achiral T_b, and final T_c configurations from figure 1. The mirror antipodes have components of opposite signs $\vec{\chi}_s(T_a) = -\vec{\chi}_s(T_c)$ and the achiral configuration has all components equal to zero $\vec{\chi}_s(T_b) = \vec{0}$. The square root of the sum of the squares of the components equals the scalar em-chirality $\hat{\chi} = 0.014$.
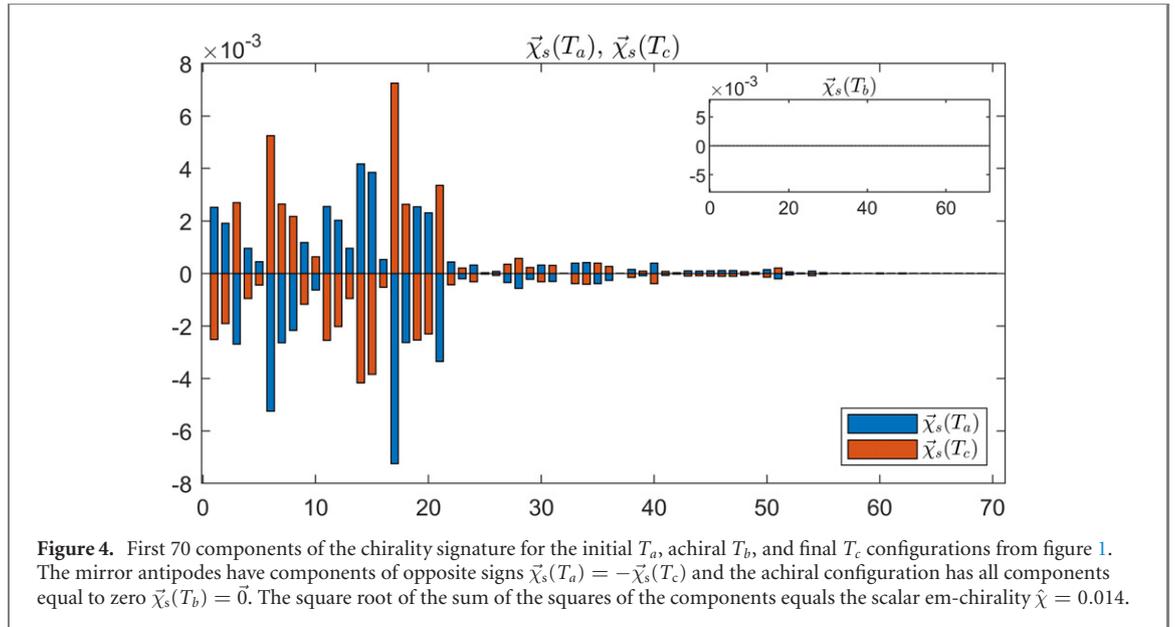
As can be seen on figure 4, the components of the chirality signature of enantiomeric configurations have opposite signs

$$\vec{\chi}_s(T_a) = -\vec{\chi}_s(T_c) \tag{51}$$

and the chirality signature of the achiral configuration has only zero components

$$\vec{\chi}_s(T_b) = \vec{0}. \tag{52}$$

An important property of the chirality signature is that its components converge to zero: it is well-known that for large enough values of multipolar order the response of spatially localized scatterers vanishes. Therefore, the matrices $T^{\lambda\lambda'}$ represent compact operators with singular values that converge to zero. This then allows to truncate the chirality signature at some point after which the contributions to the scalar em-chirality are negligible.

Each component of $\vec{\chi}_s$ acts as an independent pseudoscalar handedness measure: it changes its sign under a mirror transformation and equals zero if the object is achiral. An individual component of $\vec{\chi}_s$ sometimes equals zero for a chiral state, producing a false chiral zero. But only when *all* the elements of $\vec{\chi}_s$ equal zero, the object is em-achiral. This provides, for the first time, the concrete quantification of the infinite-dimensional nature of chirality.

We note that the chirality signature method is fundamentally different from the conventional approach, where enantiomers are distinguished by a single pseudoscalar property such as optical rotation or circular dichroism. Such properties are typically very small and can be zero for chiral objects. A property such as this one was incorporated in the phase of complex em-chirality. As one can see on figure 3, the handedness part of complex em-chirality (the real part of χ_c) is at least three orders of magnitude smaller than the corresponding scalar em-chirality (the absolute value of χ_c). This implies that the contribution of the selected pseudoscalar property to the scalar em-chirality has very low significance for our system. In fact, the handedness part of the computed χ_c is smaller than the 70'th component of the chirality signature $\vec{\chi}_s$.

The chirality signature, on the other hand, provides the complete (as defined by equations (40)–(42)) decomposition of scalar em-chirality into its pseudoscalar components. This, together with the fact that its norm $\vec{\chi}_s$ equals the scalar em-chirality $\hat{\chi}$, results in the access to significant pseudoscalar functions of the object. These are of the same order of magnitude as the scalar em-chirality, as seen on figure 4. Therefore, differentiation of enantiomers using this description is much more stable with respect to perturbations of the geometry of the object or to uncertainties in the entries of the T-matrix.

Importantly, the chirality signature is able to continuously distinguish *any* pair of enantiomers. An example of the failure of the conventional approach is the state T_u that corresponds to the chiral unhanded state $\mathfrak{R}(\chi_c) = 0$ on figure 3(b). Since the configuration is chiral, there exist its geometric enantiomer $\widetilde{T}_u$, which is a different object. But both of them acquire the same value of complex em-chirality

$$\chi_c(T_u) = \chi_c(\widetilde{T}_u). \tag{53}$$

In this case the complex em-chirality is unable to differentiate these particular enantiomers. The chirality signature, however, provides two different pseudovectors for T_u and for $\widetilde{T}_u$, as shown on figure 5.
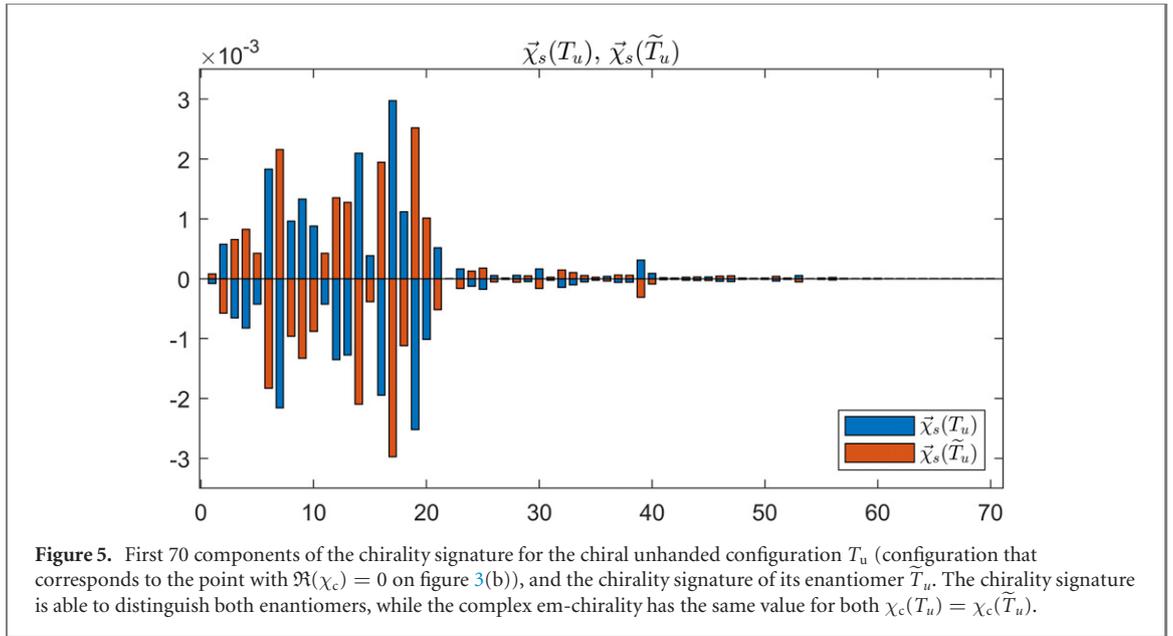
Figure 5. First 70 components of the chirality signature for the chiral unhanded configuration T_u (configuration that corresponds to the point with $\Re(\chi_c) = 0$ on figure 3(b)), and the chirality signature of its enantiomer $\widetilde{T}_u$. The chirality signature is able to distinguish both enantiomers, while the complex em-chirality has the same value for both $\chi_c(T_u) = \chi_c(\widetilde{T}_u)$.

7. Conformal invariance

The conformal group constitutes the largest symmetry group of Maxwell's equations [41]. It consists of the ten-parameter Poincaré group (four space-time translations, three rotations and three Lorentz boosts) together with a dilation and four special conformal transformations. Before proving the conformal invariance of the introduced em-chirality measures (in the polychromatic regime) we first prove their Poincaré invariance. The states (16) transform unitarily under a general Poincaré transformation X with helicity λ unchanged [32, p 198]:

$$X|\boldsymbol{p}\,\lambda\rangle = |X\boldsymbol{p}\,\lambda\rangle e^{-i\alpha(\boldsymbol{p},\lambda,X)}, \tag{54}$$

where the phase angle depends on the initial momentum, helicity, and parameters of the transformation. Each of the four scattering suboperators $T^{\lambda\lambda'}$ (defined on the whole frequency domain) will transform independently and without changing its singular values:

$$T^{\lambda\lambda'} = \sum_k \sigma_k|\psi_k\rangle\langle\phi_k| \rightarrow \sum_k \sigma_k X|\psi_k\rangle\langle\phi_k|X^\dagger = \sum_k \sigma_k|\psi_k'\rangle\langle\phi_k'|, \tag{55}$$

where $|\psi_k'\rangle = X|\psi_k\rangle$ and $|\phi_k'\rangle = X|\phi_k\rangle$ are new families of orthonormal vectors. This follows because, as previously discussed, X is unitary. It then follows from equation (26) that the norms of suboperators are invariant under X as well. This implies that the em-chirality (23), the complex em-chirality (32) and the chirality signature (47) are invariant under Poincaré transformations. We now show the conformal invariance.

As proven in [42], a massless irreducible representation of the Poincaré group can be extended to a representation of the conformal group by defining the generators of dilation and special conformal transformations as (we reproduce the equations from the original article without any changes)

$$D = \frac{1}{2}[P_0 P_k/P^2, J_{0k}]_+ \tag{56}$$

$$K_0 = \frac{1}{2}[P_0/P^2, J_{0k}J_{0k} + \Lambda^2 - 1/2]_+ \tag{57}$$

$$K_i = \frac{1}{2}[P_0/P^2, [J_{0k}, J_{ik}]_+]_+ - \frac{1}{2}[P_i/P^2, J_{0k}J_{0k} + \Lambda^2 - 1/2]_+, \tag{58}$$

where the sums over $k = 1, 2, 3$ are implied, P_μ and $J_{\mu\nu}$ are generators of the Poincaré group, Λ is the helicity operator, and $[\cdot, \cdot]_+$ is the anti-commutator.

If the Poincaré group is represented unitarily, which is our case, then the extension to the conformal group representation is also unitary [42]. Since the helicity operator Λ commutes with all elements of the Poincaré group, it is evident from equations (56)–(58) that it also commutes with all the conformal generators, which means that helicity is unchanged by conformal transformations. The singular values of T-suboperators are unchanged under the unitary conformal transformations, and we conclude that all the defined measures of em-chirality are conformally invariant. Given an object and its T-matrix, the quantities

$\chi(T)$, $\chi_c(T)$ and $\vec{\chi}_s(T)$ are the same for any conformally transformed version of the object. This means, in particular, that each $\vec{\chi}_s(T)$ is uniquely associated with a corresponding set of objects, where all objects in the set are related to each other by conformal transformations.

We note that this discussion combined with the group-theoretical representation of electromagnetic fields reveals that electromagnetic waves conserve their polarization handedness under conformal transformations. This conclusion, to the knowledge of authors, has not been previously expressed in the literature.

The fact that the results of our analysis are conformally invariant is a rare circumstance. Most physical properties, such as energy, momentum and even mass (unless it is zero) are not invariant under conformal transformations. On the contrary, the introduced chirality measures are invariant under the actions of the conformal group. Such high invariance indicates a special type of description, which only contains information that is inherent to the scatterer.

8. Applicability outside electromagnetism

We now briefly consider the applicability of the electromagnetic chirality measures to two other kinds of waves: gravitational waves, and phonons. Extension to the case of gravitational waves in linearized general relativity is straightforward because the two possible polarization modes of gravitational waves [43, sections 35.4 and 35.6] can be seen to correspond to the $\lambda = \pm 2$ massless irreducible representations of the Poincaré group. Except for the different helicity values, the situation is essentially analogous to the electromagnetic case. The applicability to chiral phonons [44–48] and mechanical chiral metamaterials [49, 50] is less straightforward. One difficulty is the existence of both transverse and longitudinal phonon waves. While the transverse waves may be mapped onto positive and negative helicity modes, the longitudinal waves are $\lambda = 0$ modes, which do not exist in the electromagnetic case. Therefore, the chirality measures discussed in this article cannot be directly applied to phonons in general. The measures could be directly applied only when both the excitation and the response of the systems involve exclusively the transverse degrees of freedom [51].

9. Final remarks

In this work, and within the context of light–matter interactions, we have solved two long-standing problems related to chirality: the false chiral zeros problem related to chiral connectedness, and the general distinction of enantiomers. We have introduced the complex electromagnetic chirality, a measure that describes the handedness of an object without acquiring false chiral zeros. We have also introduced the chirality signature of an object: an infinite-dimensional pseudovector whose components vanish simultaneously if and only if the object is electromagnetically achiral. The chirality signature provides the complete description of electromagnetic chirality, offering a continuous quantification of the multidimensional nature of chirality. Unlike conventional approaches that utilize a single pseudoscalar function, the chirality signature provides a consistent and general method for continuously distinguishing each element of any pair of enantiomers. We have proved that the scalar and complex electromagnetic chirality measures, as well as the chirality signature, are invariant under all the transformations of the conformal group. Historically, the study of invariance and symmetry concepts was often key to extending our physical understanding. The complete, continuous, and conformally invariant quantification of electromagnetic chirality provided by the chirality signature distinguishes it as a particularly suitable tool for the study of chirality and its applications. In particular, it provides a sound basis for the study of chirality evolution dynamical processes, such as chemical reactions.

Acknowledgments

Data availability statement

The data that support the findings of this study are available upon reasonable request from the authors.

Appendix A. Proof of the new formula for scalar em-chirality

First we show that, for any two Hilbert–Schmidt operators A and B, it holds that

$$\min_{U,V}\left\|A - UBV^\dagger\right\|_{\text{HS}}^2 = |\vec{\sigma}(A) - \vec{\sigma}(B)|^2, \tag{59}$$

where the minimization takes place over unitary operators U and V, $\vec{\sigma}(A)$ and $\vec{\sigma}(B)$ are non-increasing sequences of singular values, $|\vec{\sigma}(A) - \vec{\sigma}(B)|^2 = (\vec{\sigma}(A) - \vec{\sigma}(B)) \cdot (\vec{\sigma}(A) - \vec{\sigma}(B))$, and the $\cdot$ operation is defined in equation (24).

Using the Hilbert–Schmidt scalar product we re-write the left hand side as

$$\min_{U,V}\left\|A - UBV^\dagger\right\|_{\text{HS}}^2 = \tag{60}$$

$$= \min_{U,V}\langle A - UBV^\dagger,\ A - UBV^\dagger\rangle \tag{61}$$

$$= \min_{U,V}\left\{\langle A, A\rangle + \langle UBV^\dagger, UBV^\dagger\rangle - \langle A, UBV^\dagger\rangle - \langle UBV^\dagger, A\rangle\right\} \tag{62}$$

$$= \|A\|_{\text{HS}}^2 + \left\|UBV^\dagger\right\|_{\text{HS}}^2 - \max_{U,V}\left\{\langle UBV^\dagger, A\rangle + \langle A, UBV^\dagger\rangle\right\} \tag{63}$$

$$= \|A\|_{\text{HS}}^2 + \|B\|_{\text{HS}}^2 - 2\max_{U,V}\left\{\text{Re}\langle A, UBV^\dagger\rangle\right\}, \tag{64}$$

and the problem reduces to maximizing $\text{Re}\langle A, UBV^\dagger\rangle$. The von Neumann trace inequality for Hilbert–Schmidt operators states [37] that any two Hilbert–Schmidt operators X, Y fulfill the condition

$$\text{Re}\langle X, Y\rangle \leqslant \sum_{k=1}^{\infty}\sigma_k(X)\sigma_k(Y) \tag{65}$$

with equality holding if and only if X and Y share singular vectors. It is always possible to find such unitary U and V that transform the singular vectors of B onto those of A by the following construction. Consider SVDs of A and B

$$A = U_a\Sigma_a V_a^\dagger \tag{66}$$

$$B = U_b\Sigma_b V_b^\dagger. \tag{67}$$

Then for

$$U := U_a U_b^\dagger \tag{68}$$

$$V := V_a V_b^\dagger \tag{69}$$

one gets

$$UBV^\dagger = U_a U_b^\dagger U_b\Sigma_b V_b^\dagger(V_a V_b^\dagger)^\dagger = U_a\Sigma_b V_a^\dagger, \tag{70}$$

which according to the von Neumann trace inequality realizes the maximal value

$$\max_{U,V}\left\{\text{Re}\langle A, UBV\rangle\right\} = \sum_{k=1}^{\infty}\sigma_k(A)\sigma_k(B) = \vec{\sigma}(A) \cdot \vec{\sigma}(B). \tag{71}$$

Now, using $\|A\|_{\text{HS}}^2 = \vec{\sigma}(A) \cdot \vec{\sigma}(A) := \vec{\sigma}^2(A)$, where a shorthand notation is introduced after the $:=$ symbol, and, similarly $\|B\|_{\text{HS}}^2 = \vec{\sigma}^2(B)$, we finally write equation (64) as

$$\min_{U,V}\left\|A - UBV^\dagger\right\|_{\text{HS}}^2 = \vec{\sigma}^2(A) + \vec{\sigma}^2(B) - 2\,\vec{\sigma}(A) \cdot \vec{\sigma}(B) \tag{72}$$

$$= |\vec{\sigma}(A) - \vec{\sigma}(B)|^2. \tag{73}$$

Application of this formula to the definition of the scalar em-chirality (23) results in

$$\chi^2(T) = \left|\vec{\sigma}(T^{++}) - \vec{\sigma}(T^{--})\right|^2 + \left|\vec{\sigma}(T^{+-}) - \vec{\sigma}(T^{-+})\right|^2 \tag{74}$$

$$= \min_{U_1 V_1}\|T^{++} - U_1 T^{--} V_1\|_{\text{HS}}^2 + \min_{U_2 V_2}\|T^{-+} - U_2 T^{+-} V_2\|_{\text{HS}}^2, \tag{75}$$

which provides a new perspective on scalar em-chirality as the solution to a minimization problem. One can recognize a close resemblance to the well-known orthogonal Procrustes problem [52], but formulated

for Hilbert–Schmidt operators acting on the space of solutions to Maxwell's equations. The definition of em-chirality in equation (75) lends itself to straightforward formulations of T-matrix-based scalar measures of geometrical chirality. It suffices to restrict the U_i/V_i to compositions of rotations and translations. Such an approach was studied in [53].

Appendix B. Further properties of complex em-chirality

Consider a scatterer that is transparent to fields of positive helicity. Then, as was mentioned in section 3, it exhibits the maximal scalar em-chirality $\hat{\chi} = 1 = |\chi_c|$. The phase (34) can be found using

$$\left\| T^{++} \right\|^2 = \left\| T^{-+} \right\|^2 = 0, \tag{76}$$

which implies $\phi = \pi$ and it follows that the object is maximally right-handed

$$\chi_c(T) = -1. \tag{77}$$

In the case of transparency to fields of negative helicity we similarly have $\chi = 1$ together with

$$\left\| T^{--} \right\|^2 = \left\| T^{+-} \right\|^2 = 0, \tag{78}$$

so $\phi = 0$ and the object is maximally left-handed

$$\chi_c(T) = 1. \tag{79}$$

The converse is true for reciprocal objects. Assuming maximal scalar em-chirality $\hat{\chi} = 1 = |\chi_c|$ and the condition (31), we get for the normalized version of the definition (23)

$$1 = \frac{(\vec{\sigma}(T^{++}) - \vec{\sigma}(T^{--}))^2}{\vec{\sigma}(T^{++})^2 + \vec{\sigma}(T^{+-})^2 + \vec{\sigma}(T^{-+})^2 + \vec{\sigma}(T^{--})^2} \tag{80}$$

and therefore

$$\vec{\sigma}(T^{+-})^2 + \vec{\sigma}(T^{-+})^2 = -2\,\vec{\sigma}(T^{++}) \cdot \vec{\sigma}(T^{--}), \tag{81}$$

where the dot product denotes $\sum_{k=1}^{\infty} \sigma_k(T^{++})\sigma_k(T^{--})$. Since singular values are non-negative, there exist only two possibilities for this condition to be fulfilled: either

$$\vec{\sigma}(T^{+-}) = \vec{0}, \qquad \vec{\sigma}(T^{-+}) = \vec{0}, \qquad \vec{\sigma}(T^{++}) = \vec{0} \tag{82}$$

or

$$\vec{\sigma}(T^{+-}) = \vec{0}, \qquad \vec{\sigma}(T^{-+}) = \vec{0}, \qquad \vec{\sigma}(T^{--}) = \vec{0}. \tag{83}$$

If all singular values of an operator are zero, then the operator itself is zero, hence both cases signify invisibility to fields of positive and negative helicity respectively. The first case (82) implies $\phi = \pi$ and consequently the object is maximally right-handed $\chi_c = -1$, the second case (83) results in $\phi = 0$ and the maximal left-handedness $\chi_c = 1$ follows.

ORCID iDs

Maxim Vavilin ⬤ https://orcid.org/0000-0002-6361-3408
Ivan Fernandez-Corbaton ⬤ https://orcid.org/0000-0003-2834-5572

References

[1] Weinberg N and Mislow K 2000 On chirality measures and chirality properties *Can. J. Chem.* **78** 41–5
[2] Avnir D and Pinto Y 2001 A generalized handedness strategy: addressing latent handedness in chiral structures *Enantiomer* **6** 211–7
[3] Mezey P 1995 Rules on chiral and achiral molecular transformations *J. Math. Chem.* **17** 185–202
[4] Weinberg N and Mislow K 1997 On chiral pathways in $E(n)$: a dimensional analysis *Theor. Chim. Acta* **95** 63–5
[5] Ruch E 1972 Algebraic aspects of the chirality phenomenon in chemistry *Acc. Chem. Res.* **5** 49–56
[6] Waterman P C 1965 Matrix formulation of electromagnetic scattering *Proc. IEEE* **53** 805–12
[7] Mishchenko M I, Travis L D and Mackowski D W 1996 T-matrix computations of light scattering by nonspherical particles: a review *J. Quant. Spectrosc. Radiat. Transfer* **55** 535–75
[8] Wriedt T and Hellmers J 2021 *Compilation of T-matrix codes from many authors* (https://scattport.org/index.php/programs-menu/t-matrix-codes-menu) accessed 28-10-2021

[9] Fernandez-Corbaton I, Beutel D, Rockstuhl C, Pausch A and Klopper W 2020 Computation of electromagnetic properties of molecular ensembles *ChemPhysChem* **21** 878–87

[10] Fernandez-Corbaton I, Fruhnert M and Rockstuhl C 2016 Objects of maximum electromagnetic chirality *Phys. Rev. X* **6** 031013

[11] Gorkunov M V, Antonov A A and Kivshar Y S 2020 Metasurfaces with maximum chirality empowered by bound states in the continuum *Phys. Rev. Lett.* **125** 093903

[12] Arens T, Griesmaier R and Knöller M 2021 Maximizing the electromagnetic chirality of thin dielectric tubes *SIAM J. Appl. Math.* **81** 1979–2006

[13] Garcia-Santiago X *et al* 2021 Towards maximal electromagnetically chiral scatterers at optical frequencies (arXiv:2112.04422) accessed 02 03 2022 (under review)

[14] Arens T, Hagemann F, Frank H and Kirsch A 2018 The definition and measurement of electromagnetic chirality *Math. Methods Appl. Sci.* **41** 559–72

[15] Stratis I G 2021 Chirality notions and electromagnetic scattering: a mini review *Complex Variables and Elliptic Equations* 1–33

[16] Feringa B L and van Delden R A 1999 Absolute asymmetric synthesis: the origin, control, and amplification of chirality *Angew. Chem., Int. Ed.* **38** 3418–38

[17] Reetz M T and Garcia-Borràs M 2021 The unexplored importance of fleeting chiral intermediates in enzyme-catalyzed reactions *J. Am. Chem. Soc.* **143** 14939–50

[18] Fernandez-Corbaton I, Vidal X, Tischler N and Molina-Terriza G 2013 Necessary symmetry conditions for the rotation of light *J. Chem. Phys.* **138** 214311

[19] Canaguier-Durand A, Hutchison J A, Genet C and Ebbesen T W 2013 Mechanical separation of chiral dipoles by chiral light *New J. Phys.* **15** 123037

[20] Coles M M, Williams M D, Saadi K, Bradshaw D S and Andrews D L 2013 Chiral nanoemitter array: a launchpad for optical vortices *Laser Photon. Rev.* **7** 1088–92

[21] Bliokh K Y, Kivshar Y S and Nori F 2014 Magnetoelectric effects in local light–matter interactions *Phys. Rev. Lett.* **113** 033601

[22] Cameron R P, Barnett S M and Yao A M 2014 Discriminatory optical force for chiral molecules *New J. Phys.* **16** 013020

[23] Efrati E and Irvine W T M 2014 Orientation-dependent handedness and chiral design *Phys. Rev. X* **4** 011003

[24] Nieto-Vesperinas M 2015 Optical theorem for the conservation of electromagnetic helicity: significance for molecular energy transfer and enantiomeric discrimination by circular dichroism *Phys. Rev. A* **92** 023813

[25] Poulikakos L V, Gutsche P, McPeak K M, Burger S, Niegemann J, Hafner C and Norris D J 2016 Optical chirality flux as a useful far-field probe of chiral near fields *ACS Photon.* **3** 1619–25

[26] Andrews D 2018 Symmetries, conserved properties, tensor representations, and irreducible forms in molecular quantum electrodynamics *Symmetry* **10** 298

[27] Philipp G and Manuel N-V 2018 Optical chirality of time-harmonic wavefields for classification of scatterers *Sci. Rep.* **8** 9416

[28] Crimin F, Mackinnon N, Götte J B and Barnett S M 2019 On the conservation of helicity in a chiral medium *J. Opt.* **21** 094003

[29] Poulikakos L, Dionne J and García-Etxarri A 2019 Optical helicity and optical chirality in free space and in the presence of matter *Symmetry* **11** 1113

[30] Hanifeh M, Albooyeh M and Capolino F 2020 Optimally chiral light: upper bound of helicity density of structured light for chirality detection of matter at nanoscale *ACS Photon.* **7** 2682–91

[31] Fernandez-Corbaton I 2021 Total helicity of electromagnetic fields and matter *Phys. Rev. B* **103** 054406

[32] Tung W-K 1985 *Group Theory in Physics* (Singapore: World Scientific)

[33] Jackson J D 1999 *Classical Electrodynamics* 3rd edn (New York: Wiley)

[34] Moses H E 1973 Photon wave functions and the exact electromagnetic matrix elements for hydrogenic atoms *Phys. Rev. A* **8** 1710–21

[35] Peterson B and Ström S 1973 *T*-matrix for electromagnetic scattering from an arbitrary number of scatterers and representations of *E*(3) *Phys. Rev. D* **8** 3661

[36] Gross L 1964 Norm invariance of mass-zero equations under the conformal group *J. Math. Phys.* **5** 687–95

[37] Carlsson M 2021 von Neumann's trace inequality for Hilbert–Schmidt operators *Expo. Math.* **39** 149–57

[38] Sapienza R 2005 Photonic nano materials: anisotropic transport and optical Bloch oscillations *PhD Thesis* Université Pierre et Marie Curie-Paris VI

[39] Mishchenko M I 2020 Comprehensive thematic *T*-matrix reference database: a 2017–2019 update *J. Quant. Spectrosc. Radiat. Transfer* **242** 106692

[40] Beutel D, Groner A, Rockstuhl C and Fernandez-Corbaton I 2021 Efficient simulation of biperiodic, layered structures based on the *T*-matrix method *J. Opt. Soc. Am. B* **38** 1782–91

[41] Gilmore R 1974 *Lie Groups, Lie Algebras, and Some of Their Applications* (Hoboken, NJ: Wiley)

[42] Fushchich V I and Nikitin A G 1978 Conformal invariance of relativistic equations for arbitrary spin particles *Lett. Math. Phys.* **2** 471–5

[43] Misner C W, Thorne K S and Wheeler J A 1973 *Gravitation* (San Francisco, CA: Freeman)

[44] Zhang L and Niu Q 2014 Angular momentum of phonons and the Einstein–de Haas effect *Phys. Rev. Lett.* **112** 085503

[45] Gao M, Zhang W and Zhang L 2018 Nondegenerate chiral phonons in graphene/hexagonal boron nitride heterostructure from first-principles calculations *Nano Lett.* **18** 4424–30

[46] Zhu H *et al* 2018 Observation of chiral phonons *Science* **359** 579–82

[47] Chen H, Wu W, Zhu J, Yang S A and Zhang L 2021 Propagating chiral phonons in three-dimensional materials *Nano Lett.* **21** 3060–5 PMID:33764075

[48] Chen Y, Frenzel T, Zhang Q, Kadic M and Wegener M 2021 Cubic metamaterial crystal supporting broadband isotropic chiral phonons *Phys. Rev. Mater.* **5** 025201

[49] Kadic M, Milton G W, van Hecke M and Wegener M 2019 3D metamaterials *Nat. Rev. Phys.* **1** 198–210

[50] Chen Y, Kadic M and Wegener M 2021 Chiral triclinic metamaterial crystals supporting isotropic acoustical activity and isotropic chiral phonons *Proc. R. Soc. A* **477** 20200764

[51] Iglesias Martínez J A, Groß M F, Chen Y, Frenzel T, Laude V, Kadic M and Wegener M 2021 Experimental observation of roton-like dispersion relations in metamaterials *Sci. Adv.* **7** eabm2189

[52] Gower J C and Dijksterhuis G B 2004 *Procrustes Problems* (Oxford: Oxford University Press) on demand

[53] Gutsche P, Garcia-Santiago X, Schneider P-I, McPeak K M, Nieto-Vesperinas M and Burger S 2020 Role of geometric shape in chiral optics *Symmetry* **12** 158